Monthly Notices
of the
ROYAL ASTRONOMICAL SOCIETY

MNRAS **487,** 729–736 (2019) doi:10.1093/mnras/stz1229

Fourier-series expansion of the dark-energy equation of state

David Tamayo[1]★ and J. Alberto Vázquez[2]

[1]*Departamento de Física, Centro de Investigación y de Estudios Avanzados del IPN, A.P. 14-740, 07000 Mexico City., Mexico.*
[2]*Instituto de Ciencias Físicas, Universidad Nacional Autonoma de México, Apdo. Postal 48-3, 62251 Cuernavaca, Morelos, Mexico.*

Accepted 2019 April 29. Received 2019 April 22; in original form 2019 February 27

ABSTRACT

The dark-energy component of the Universe still remains a mystery; however, several papers based on observational data have shown that its equation of state may have an oscillatory behaviour. In this paper, we provide a general description for the dark-energy equation of state $w(z)$ in the form of a Fourier series. This description generalizes some previous dynamical dark-energy models and is in agreement with the $w(z)$ reconstructions. We make use of a modified version of a simple and fast Markov chain Monte Carlo code to constrain the model parameters. For the analysis we use data from supernovae type Ia, baryon acoustic oscillations, $H(z)$ measurements and cosmic microwave background. We provide a comparison of the proposed model with ΛCDM, wCDM and the standard Taylor approximation. The Fourier-series expansion of $w(z)$ is preferred from ΛCDM at more than the 3σ significance level based on the improvement in the fit alone. We use the Akaike criterion to perform the model comparison and find that, even though there are extra parameters, there is a slight preference for the Fourier series compared with the ΛCDM model. The preferred shape of $w(z)$ found here puts in jeopardy the single scalar field models, as they cannot reproduce the crossing of the phantom divide line $w = -1$.

Key words: cosmology – dark energy.

1 INTRODUCTION

Dark energy is still an unknown negative-pressure cosmic component for which the simplest case is given in terms of a perfect fluid with an equation of state (EoS) $p = w\rho$ with $w = -1$; this particular model is commonly called the cosmological constant Λ and it is a key piece of the standard cosmological model, the ΛCDM model. Even though the standard cosmological model fits well with most of the current astronomical observations, there exist important tensions between different recent data sets. For instance, the value of H_0 measured from cosmic microwave background (CMB) data by the Planck Collaboration (Ade et al. 2016) is 3.4σ lower than the local value reported by Riess et al. (2016). The matter density fraction consistent with the Lyman α forest measurement of the baryon acoustic oscillations (BAO) is smaller than the one preferred by CMB measurements (Delubac et al. 2015). On the other hand, based on the most minimal a priori assumptions, model-independent reconstructions of the evolution of the dark-energy EoS parameter exhibit a dynamical behaviour of $w(z)$ (Alberto Vazquez et al. 2012; Zhao et al. 2017; Hee et al. 2017; Wang et al. 2018), putting in tension the ΛCDM model amongst several models for which $w =$ constant. From the theoretical point of view, the standard cosmological model also carries several important theoretical problems such as the absence of physical grounds to justify the cosmological constant, the coincidence problem and fine-tuning (see Velten, vom Marttens & Zimdahl 2014; Padilla 2015; López-Corredoira 2017). In order to get around these issues, there have been plenty of proposals to describe the general behaviour of this dark component, i.e. scalar fields (quintessence, K-essence, phantom, quintom, non-minimally coupled scalar fields, etc.) (Arun, Gudennavar & Sivaram 2017), modified gravity (Clifton et al. 2012), interacting dark energy (Zimdahl 2012) and divergence free parametrizations (Akarsu, Dereli & Vazquez 2015), among many others (Yoo & Watanabe 2012).

Dark-energy parametrizations of the EoS parameter are a set of phenomenological models that consist of assuming that the dark energy behaves as a perfect fluid with a dynamical equation of state, that is, $p = w(z)\rho$, without any other assumption about the origin of this behaviour from fundamental physics. The main goal of this approach is to model the time evolution of $w(z(t))$ from observational data, which can give important insights into the evolution of the dark energy and set a phenomenological basis for its theoretical description. Here we briefly summarize some of these models.

★ E-mail: tamayo.ramirez.d.a@gmail.com

First, one of the most popular time-evolving parametrizations consists of expanding w in a Taylor series around $a = 1$ (today): $w(a) = \sum_{i=0}^{N}(1-a)^i w_i$, where N defines the order of the polynomial expansion and w_i are constant values. The trivial case, when $N = 0$, is $w(a) = w_0$, also known as the wCDM model, and for the particular case of $w_0 = -1$ we clearly return to the well-known cosmological constant. The case $N = 1$, i.e. $w(a) = w_0 + (1-a)w_1$, corresponds to the very well-known Chevallier–Polarski–Linder (CPL) model (Chevallier & Polarski 2001; Linder 2003); this richer model has been widely studied (Kumar & Xu 2014) and can be mapped into other dark-energy models like quintessence and barotropic dark energy (Scherrer 2015). A recent study of several cases of the wCDM and CPL models can be found in Sagredo, Lafaurie & Sapone (2018); here the authors compare the models by performing different statistical criteria in order to highlight the differences. For higher orders $N = 2, 3, 4$, a nice analysis is performed in Dai, Yang & Xia (2018); by analysing cosmological data (supernovae type Ia (SNIa), CMB, Large Scale Structure (LSS), $H(z)$, BAO) the authors conclude that the concordance cosmological constant model ($w = -1$) is still safely consistent with these observational data at the 68 per cent confidence level. However, when adding the high-redshift BAO measurement from the Lyα forest of BOSS DR11 quasars into the calculation there is a significant impact on the reconstruction result: the w prefers values significantly smaller than -1.

Parametrizations that use power laws and exponential functions with two and three free parameters were analysed by Martins et al. in Martins & Colomer (2018). Through a standard statistical analysis of cosmological data (SNIa, $H(z)$) they set constraints at the present-day values of the dark-energy EoS and in the asymptotic past in these models. They conclude that the dark-energy EoS near the present day must be very similar to that of a cosmological constant, and any significant deviations from this behaviour can only occur in the deep-matter era.

Another approach consists in phenomenological models using trigonometric functions. A first attempt was proposed by Linder arguing that oscillating dark-energy models offer one idea for solving the coincidence problem (Linder 2006): the ansatz considers an EoS parameter with the form of $w(a) = w_0 - A\sin(B\ln a)$ where the natural period of the cosmic expansion is given by $H^{-1} = (\mathrm{d}\ln a/\mathrm{d}t)^{-1}$, so they examine periodicity in units of the e-folding scale $\ln a$. A further work by Pace et al. (2012) studies the imprints on the formation and evolution of cosmic structures in six different variations of this particular dark-energy model. Moreover, from a phantom scalar field conformally coupled to a gravity model, Kurek et al. obtain a parametrization of the type $w(z) = -1 + (1+z)^3[C_1\cos(\ln(1+z)) + C_2\sin(\ln(1+z))]$ (Kurek, Hrycyna & Szydlowski 2008). Pan, Saridakis & Yang (2018) study several oscillating dark-energy models: $w_{\rm I} = w_0 + b[1-\cos(\ln(1+z))]$, $w_{\rm II} = w_0 + b\sin(\ln(1+z))$, $w_{\rm III} = w_0 + b[\frac{\sin(1+z)}{1+z} - \sin 1]$ and $w_{\rm IV} = w_0 + b[\frac{z}{1+z}\cos(1+z)]$; see references therein to see the motivation behind the selection of these particular phenomenological models. They perform a comparison of these dark-energy parametrizations with observational data (Joint Light-curve Analysis (JLA), SNIa, BAO, CMB, redshift space distortion, weak gravitational lensing, $H(z)$) and find that the best-fitting characters of almost all the models are bent towards the phantom region; nevertheless, in all of them, the quintessential regime is also allowed within the 1σ confidence level. Finally, they perform a Bayesian analysis, which shows that the current observational data support the ΛCDM paradigm over this set of oscillating dark-energy parametrizations. A complementary study for this set of models is done in Panotopoulos & Rincón (2018), where the authors compute the statefinder parameters, and at the level of linear cosmological perturbations they compute the growth index as well as the combination parameter $f\sigma_8$, obtaining similar conclusions. Jaime, Jaber & Escamilla-Rivera (2018) propose a cosine-like parametrization for the dark-energy EoS with the form $w = -1 + \frac{w_0}{1+w_1 z^{w_2}}\cos(w_3 + z)$, which can reproduce some successful $f(R)$ gravity models with a precision between 0.5 and 0.8 per cent over the numerical solutions; using observational data from BAO, SNIa, and cosmic chronometers, they investigate the constraints on the new EoS parameters.

The aforementioned reconstruction of $w(z)$ from observational data shows that the shape of $w(z)$ crosses the phantom divide line (PDL) $w = -1$ several times, having an oscillating behaviour, and puts in jeopardy many dark-energy models such as ΛCDM and single scalar field models that are unable to cross the PDL. This oscillating $w(z)$ can be modelled with a Taylor series of third order or more, but has its limitations: first, the expansion has to be done around a specific point that is commonly around $z = 0$ and this implies that far away from the expansion point the approximation may not be accurate; secondly, the expansion is done with polynomials and to describe an oscillatory function many terms are needed to get a good representation; and thirdly, sufficiently far from $z = 0$ the polynomial always grows or decreases monotonically.

If we want to model an oscillating $w(z)$, trigonometric functions are a natural choice and therefore in this work we generalize this idea using a general description of $w(z)$ in the form of a Fourier series. This approach avoids the Taylor-expansion problems mentioned before: the expansion is done over a period and not a point, fewer terms of the series are needed to reproduce well the oscillations, and the trigonometric functions are bounded. We show that the Fourier-series approach fits the data better than the Taylor-expansion models.

The present work is organized in the following way: first, in Section 2 we provide a general description of the model proposed in this work. Then in Section 3 the methodology of the data analysis is done. The results and constraints of the proposed models as well as its comparison with different models are shown in Section 4. Finally the conclusion and discussion of the results are presented in Section 5.

2 THE OSCILLATING DARK-ENERGY MODEL

The general idea of this work is to consider the EoS parameter $w(a)$ as a Fourier series in the interval $1 \geq a \geq a_{\rm med}$ (remembering the convention of the value of the scale factor at the present time $a(t_0) \equiv 1$), a linear adjustment in the interval $a_{\rm med} \geq a \geq a_{\rm ini}$ and $w = -1$ otherwise. The motivation behind selecting these intervals is the following. First, the available data show a possible oscillating behaviour of w at low redshifts ($0 \leq z \lesssim 2.5$) (Zhao et al. 2017), thus the first natural approximation is to use trigonometric functions and then in a more

general form use the Fourier series. Then, at higher redshifts ($z \gtrsim 3$) there is not enough evidence about the behaviour of w different from the cosmological constant, i.e. we use $w = -1$. To join these two different behaviours in a continuous way we use a transitional interval in which w is linear. We impose that at the transition points, $a_{\rm med}$ and $a_{\rm ini}$, the value of the functions used by our model is continuous, $w_{\rm F}(a_{\rm med}) = w_{\rm L}(a_{\rm med})$ and $w_{\rm L}(a_{\rm ini}) = w_{\rm C} = -1$, where the subscripts F, L, C correspond to the Fourier, linear and constant parts of w. Therefore, the piecewise function of the EoS parameter w in terms of the scale factor is:

$$w(a) = \begin{cases} -1 & a_{\rm ini} > a, \\ m\,(a - a_{\rm ini}) + b & a_{\rm med} \geq a \geq a_{\rm ini}, \\ \dfrac{w_0}{2} + \displaystyle\sum_{n=1}^{\infty} \left(a_n \sin\left[\dfrac{2n\pi}{T}(a - a_{\rm med})\right] + b_n \cos\left[\dfrac{2n\pi}{T}(a - a_{\rm med})\right]\right) & 1 \geq a \geq a_{\rm med}. \end{cases} \tag{1}$$

In terms of the redshift $a = (z + 1)^{-1}$ we have

$$w(z) = \begin{cases} -1 & z_{\rm ini} < z, \\ m\left(\frac{1}{z+1} - \frac{1}{z_{\rm ini}+1}\right) + b & z_{\rm med} \leq z \leq z_{\rm ini}, \\ \frac{w_0}{2} + \sum_{n=1}^{\infty} \left(a_n \sin\left[\frac{2n\pi}{T}\left(\frac{1}{z+1} - \frac{1}{z_{\rm med}+1}\right)\right] + b_n \cos\left[\frac{2n\pi}{T}\left(\frac{1}{z+1} - \frac{1}{z_{\rm med}+1}\right)\right]\right) & 0 \leq z \leq z_{\rm med}, \end{cases} \tag{2}$$

where $T = 1 - a_{\rm med}$ is the period. The constants of the linear equation, m and b, can be calculated from the equation of a line given two points (P_1, P_2):

$$P_1 = (a_{\rm med},\ w(a_{\rm med})) \equiv (a_{\rm med},\ w_{\rm med}) = \left(a_{\rm med},\ \frac{w_0}{2} + \sum_{n=1}^{\infty} b_n\right), \tag{3}$$

$$P_2 = (a_{\rm ini},\ w(a_{\rm ini})) \equiv (a_{\rm ini},\ w_{\rm ini}) = (a_{\rm med},\ -1); \tag{4}$$

therefore

$$m = \frac{w_{\rm med} - w_{\rm ini}}{a_{\rm med} - a_{\rm ini}} = \frac{\frac{w_0}{2} + \sum_n b_n + 1}{a_{\rm med} - a_{\rm ini}}, \tag{5}$$

$$b = w_{\rm ini} = -1. \tag{6}$$

To calculate the dark-energy density $\rho_{\rm de}$ we have to solve the conservation equation

$$\dot{\rho}_{\rm de} + 3H(1 + w)\rho_{\rm de} = 0, \tag{7}$$

$$\Rightarrow \quad \rho_{\rm de} = A\, \exp\left[-3 \int (1 + w) \frac{{\rm d}a}{a}\right], \tag{8}$$

where A is the integration constant. Performing the integral for the different parts of $w(a)$ we have:

$$\rho_{\rm F} = A_{\rm F}\, a^{-3(1+\frac{w_0}{2})}\, \exp\left[-3 \sum_{n=1}^{\infty} {\rm Ci}(a\, n\theta)[b_n \cos(a_{\rm med} n\theta) - a_n \sin(a_{\rm med} n\theta)]\right] \times \exp\left[-3 \sum_{n=1}^{\infty} {\rm Si}(a\, n\theta)[a_n \cos(a_{\rm med} n\theta) + b_n \sin(a_{\rm med} n\theta)]\right], \tag{9}$$

$$\rho_{\rm L} = A_{\rm L}\, a^{1+b+3m\,a_{\rm ini}} {\rm e}^{3m\,a}, \tag{10}$$

$$\rho_{\rm C} = A_{\rm C}, \tag{11}$$

where $A_{\rm F}$, $A_{\rm L}$, $A_{\rm C}$ are the integration constants for each particular case, $\theta = 2\pi/T$, and Ci and Si are the cosine integral and sine integral, defined as:

$${\rm Ci}(x) = -\int_x^{\infty} \frac{\cos t}{t}\, {\rm d}t, \quad {\rm Si}(x) = \int_0^x \frac{\sin t}{t}\, {\rm d}t, \tag{12}$$

which in the interval $1 \geq a \geq a_{\rm med}$ are well defined. The integration constants are calculated by solving the system $\rho_{\rm F}(a_{\rm med}) = \rho_{\rm L}(a_{\rm med})$, $\rho_{\rm L}(a_{\rm ini}) = \rho_{\rm C}(a_{\rm ini})$ and to close the system we use $\rho_{\rm F}(a(t_0)) \equiv \rho_0$ (the energy density of the dark energy today). Solving this, we obtain the integration constants:

$$A_{\rm F} = \rho_{\rm de}^{(0)} \exp\left[3 \sum_{n=1}^{\infty} [{\rm Ci}(n\theta) f_n + {\rm Si}(n\theta) g_n]\right], \tag{13}$$

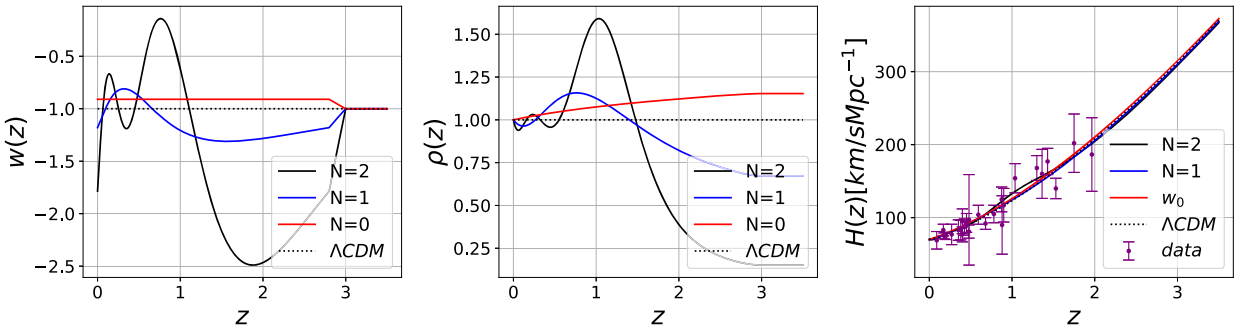

Figure 1. Left: dark-energy EoS parameter $w(z)$; middle: energy density $\rho(z)$ of the dark energy; and right: Hubble function $H(z)$ with data from Gómez-Valent & Amendola (2018). The solid black and blue lines show the first two harmonics of the Fourier series $N = 2, 1$ (the number of pairs of a_n and b_n of the expansion), the red line shows the case with only the constant term w_0 of the series and the dotted black line corresponds to the ΛCDM model. The values of a_n, b_n and w_0 used for this plot were taken from Table 1.

$$A_{\rm L} = A_{\rm F}\, a_{\rm med}^{-3(\frac{w_0}{2}-b+a_{\rm ini}m)} \exp\left[3\sum_{n=1}^{\infty}[a_{\rm med}m - f_n\,{\rm Ci}(a_{\rm med}\,n\theta) - g_n\,{\rm Si}(a_{\rm med}\,n\theta)]\right], \tag{14}$$

$$A_{\rm C} = A_{\rm L}\, a_{\rm ini}^{-3(1+b-a_{\rm ini}m)} {\rm e}^{-3a_{\rm ini}m}, \tag{15}$$

where $\rho_{\rm de}^{(0)} = \rho_{\rm de}(a = 1)$ and we have defined the auxiliary functions

$$f_n = b_n \cos(a_{\rm med}\,n\theta) - a_n \sin(a_{\rm med}\,n\theta), \tag{16}$$

$$g_n = a_n \cos(a_{\rm med}\,n\theta) + b_n \sin(a_{\rm med}\,n\theta). \tag{17}$$

Given the energy density of the dark energy, we can calculate the Hubble function for a cosmological model of a universe filled with matter (baryonic and dark matter), radiation (photons, neutrinos, etc.) and dark energy:

$$H = H_0\left(\Omega_{\rm m}^{(0)}a^{-3} + \Omega_{\rm r}^{(0)}a^{-4} + \Omega_{\rm de}^{(0)}\,\rho_{\rm de}/\rho_{\rm de}^{(0)}\right)^{1/2}, \tag{18}$$

remembering that $\Omega_i = \rho_i/\rho_{\rm crit}$ for the ith commponent, $\rho_{\rm crit}$ is the critical density of the Universe and $\Omega_i^{(0)} = \rho_i^{(0)}/\rho_{\rm crit}^{(0)} = (8\pi G/3H_0^2)\rho_i^{(0)}$. As an example, Fig. 1 displays $w(z)$, $\rho(z)$ and $H(z)$ for the first two harmonics of the Fourier series, the constant case and ΛCDM.

3 METHOLOGY

In order to perform the parameter-space exploration, and select the best-fitting model, we make use of a modified version of a simple and fast Markov chain Monte Carlo (MCMC) code that computes expansion rates and distances from the Friedmann equation, called SIMPLEMC (Aubourg et al. 2015; Slosar 2014). The data sets considered throughout the analysis include a compressed version of the Planck data (PLK), a recent reanalysis of SNIa data, and high-precision BAO measurements at different redshifts up to $z < 2.36$ (Aubourg et al. 2015). We also include a collection of currently available $H(z)$ measurements (HD); see Gómez-Valent & Amendola (2018) and references therein. We assume a flat ΛCDM universe described by the following parameters: $\Omega_{\rm b}\,h^2$ and $\Omega_{\rm DM}$ are the physical baryon density and dark matter density, respectively, relative to the critical density, and h the dimensionless Hubble parameter such that $H_0 = 100\,h\ {\rm s}^{-1}\ {\rm Mpc}^{-1}$ km. Here the neutrinos are massless and the effective number of relativistic species has the standard ΛCDM value of $N_{\rm eff} = 3.04$. The code neglects perturbations for the dark energy, but this could be an important point to deal with in future work. The SIMPLEMC code contains the Gelman–Rubin convergence criterion (R), which is typically set up to be $0.97 < R < 1.03$; for an extended review of cosmological parameter inference in cosmology see Padilla et al. (2019). In our Fourier description we introduce a set of free parameters w_0, a_n, b_n to describe the overall shape of the dark-energy equation of state $w(z)$. The transition points selected are $z_{\rm ini} = 3.0$ and $z_{\rm med} = 2.8$. For each of them, we allow variations in amplitudes with conservative flat priors $w_0 = [-3, -1]$ and $a_n, b_n = [-1.5, 1.5]$. The left-hand columns of Table 1 display the parameters used throughout each description of $w(z)$.

We perform a model comparison in order to select the best description for the equation of state $w(z)$. The main aim of the model selection is to balance the goodness of fit to the observational data against the complexity of the model, in this case given by the extra free parameters. One way to carry out this process is by calculating the Bayesian evidence, which naturally incorporates a penalization factor through the prior volume of the parameter space (Alberto Vazquez et al. 2012; Hee et al. 2017). Calculating the evidence could be challenging and a computationally demanding process. In this work, however, for simplicity and noticing the near-Gaussianity of the posterior distributions, we focus on information criteria methods such as the Akaike information criterion (AIC). The AIC is defined as:

$${\rm AIC} = -2\ln\mathcal{L}_{\rm max} + 2k, \tag{19}$$

Table 1. Constraints on the set of parameters used in each description for $w(z)$. For one-tailed distributions the upper limit 95 per cent C.L. is given and for two-tailed ones the 68 per cent one is shown. Its corresponding plot is displayed in Fig. 3. For each parametrization of $w(z)$ we have considered two sets of data: the first row contains SNIa+BAO+HD, while the second row additionally includes PLK data. The second column describes the specific model chosen in the text, with $x = \frac{2\pi}{T}(\frac{1}{z+1} - \frac{1}{z_{\rm med}+1})$.

	Model	w_0	a_1	b_1	a_2	b_2	$-2\ln\mathcal{L}_{\rm max}$	S/N[a]	$\Delta{\rm AIC_C}$
	ΛCDM	-2	0	0	0	0	68.98	0	0
		-2	0	0	0	0	73.44	0	0
(a)	$\frac{w_0}{2}$	-1.82 ± 0.12	0	0	0	0	67.06	1.4σ	0.3
		-1.93 ± 0.08	0	0	0	0	73.84	0.5σ	2.6
(b)	$w_0 + \frac{z}{1+z}a_1$[b]	-0.87 ± 0.11	-0.28 ± 0.58	0	0	0	67.08	1.4σ	2.7
		-0.94 ± 0.10	-0.11 ± 0.34	0	0	0	73.66	0.5σ	4.8
(c)	$\frac{w_0}{2} + a_1\sin(x)$	-2.06 ± 0.32	-0.16 ± 0.20	0	0	0	66.74	1.5σ	2.3
		-2.01 ± 0.12	-0.10 ± 0.11	0	0	0	73.24	0.4σ	4.4
(d)	$\frac{w_0}{2} + b_1\cos(x)$	-1.78 ± 0.13	0	-0.11 ± 0.12	0	0	66.12	1.7σ	1.7
		-1.94 ± 0.08	0	-0.06 ± 0.11	0	0	73.50	0.2σ	4.6
(e)	$\frac{w_0}{2} + a_1\sin(x)$	-2.12 ± 0.33	-0.22 ± 0.21	-0.12 ± 0.13	0	0	65.84	1.8σ	3.8
	$+b_1\cos(x)$	-2.09 ± 0.14	-0.19 ± 0.13	-0.17 ± 0.12	0	0	71.56	1.4σ	5.1
(f)	$a_1\sin(x) + b_1\cos(x)$	-2	-0.09 ± 0.08	-0.54 ± 0.23	-0.54 ± 0.27	0	61.52	2.7σ	-0.5
	$+a_2\sin(2x)$	-2	-0.07 ± 0.09	-0.26 ± 0.12	-0.27 ± 0.17	0	69.66	1.9σ	3.2
(g)	$\frac{w_0}{2} + a_1\sin(x) + b_1\cos(x)$	-2.34 ± 0.31	-0.29 ± 0.20	-0.70 ± 0.29	-0.72 ± 0.34	0	61.24	2.8σ	1.7
	$+a_2\sin(2x)$	-2.53 ± 0.24	-0.38 ± 0.17	-0.70 ± 0.23	-0.76 ± 0.28	0	63.94	3.1σ	-0.1
(h)	$\frac{w_0}{2} + a_1\sin(x) + b_1\cos(x)$	-2.31 ± 0.31	-0.28 ± 0.22	-0.65 ± 0.30	-0.67 ± 0.34	0.02 ± 0.23	61.40	2.8σ	4.4
	$+a_2\sin(2x) + b_2\cos(2x)$	-2.50 ± 0.28	-0.41 ± 0.22	-0.66 ± 0.27	-0.70 ± 0.30	0.13 ± 0.26	64.26	3.0σ	0.2

[a]Signal-to-noise ratio $= \sqrt{2\Delta\ln\mathcal{L}}$ of $w(z)$ deviating from ΛCDM based on the improvement in the fit alone.
[b]This particular model corresponds to the CPL parametrization.

where the first term incorporates the goodness of fit through the likelihood $\mathcal{L}$, and the second term is interpreted as the penalization factor given by two times the extra number of parameters (k) of the model. The more complex the model is, the faster the penalty term takes over. For a small number of data points N, it is important to attach a correction term to the AIC (Burnham & Anderson 2002), given by

$$\mathrm{AIC_C} = \mathrm{AIC} + \frac{2k(k+1)}{N-k-1}. \tag{20}$$

Therefore the preferred model is the one that minimizes $\mathrm{AIC_C}$.

4 RESULTS

Table 1 displays the mean and 1σ error values obtained during the analysis for the coefficients on each Fourier expansion. For each model the first row uses data from SNIa+BAO+HD, while the second row additionally includes PLK data. The last three columns of the table contain statistical information in order to provide an insight into the best model. Notice that some of the best-fitting values of the parameters are located right outside the ΛCDM model, within statistical significance. Of particular interest are the last three models where deviations from the standard values $a_1 = b_1 = a_2 = 0$ are more noticeable, hence leading to a significant improvement in the likelihood. For instance, model (f), with three extra parameters and fixed w_0, has deviations from ΛCDM at about 2σ according to the signal-to-noise ratio in the fit alone. Moreover, if w_0 is allowed to be a free parameter in model (g), the best fit improves significantly as a consequence of w_0 being different from the standard value $w_0 = -2$ and deviations from ΛCDM increase to up to 3σ. The inclusion of extra parameters improves the fit to the data (dashed lines in Fig. 2); however, it also carries a penalization factor that directly affects the Akaike criterion (solid lines in Fig. 2). That is, even though model (h) contains an extra parameter b_2, it has no impact on improving the fit. This is a consequence of b_2 being close to zero and hence providing no contribution to enhance the description of the data. Nevertheless, because of this increment of the number of parameters the penalty term takes over and hence the AIC value increases again. We can go even further adding parameters; however, as we have seen, the penalization factor dominates and also more freedom brings more correlations between parameters and therefore noisier reconstructions. Fig. 3 shows the posterior distribution (with 1σ and 2σ confidence levels) for the equation of state $w(z)$ given the set of MC chains for each description. As expected, adding parameters provides more structure than the cosmological constant. Let us have a look again at the last three models, where the shape of $w(z)$ resembles a similar form already obtained in previous analyses, i.e. Alberto Vazquez et al. (2012), Hee et al. (2017), Zhao et al. (2017). Throughout these reconstructions we notice the presence of two peaks, the major one located at $z \sim 0.8$ and a small one at $z \sim 0.2$ (similar positions to the ones obtained by Zhao et al. 2017). It is also observed that at the present time ($z = 0$) and high redshifts ($z > 1$) slightly favour $w < -1$, while at redshift ($z \sim 0.8$) $w > -1$ is preferred, and hence the reconstructed $w(z)$ exhibits the crossing of the PDL several times. The crossing of the PDL plays a key role in identifying the

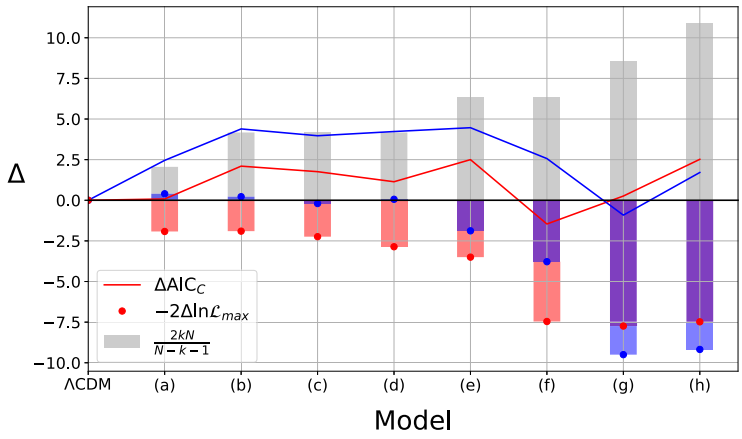

Figure 2. Red bars show that the inclusion of extra parameters improves the fit to the data, seen through $-2\Delta \ln \mathcal{L}_{\max}$ (compared to ΛCDM). We can go even further adding parameters; however, this increment causes the penalty term (grey bars) to dominate and hence the $\mathrm{AIC_C}$ value increases again. Therefore, the preferred model is the one that minimizes the $\mathrm{AIC_C}$ (solid lines). The blue bars additionally includes PLK data.

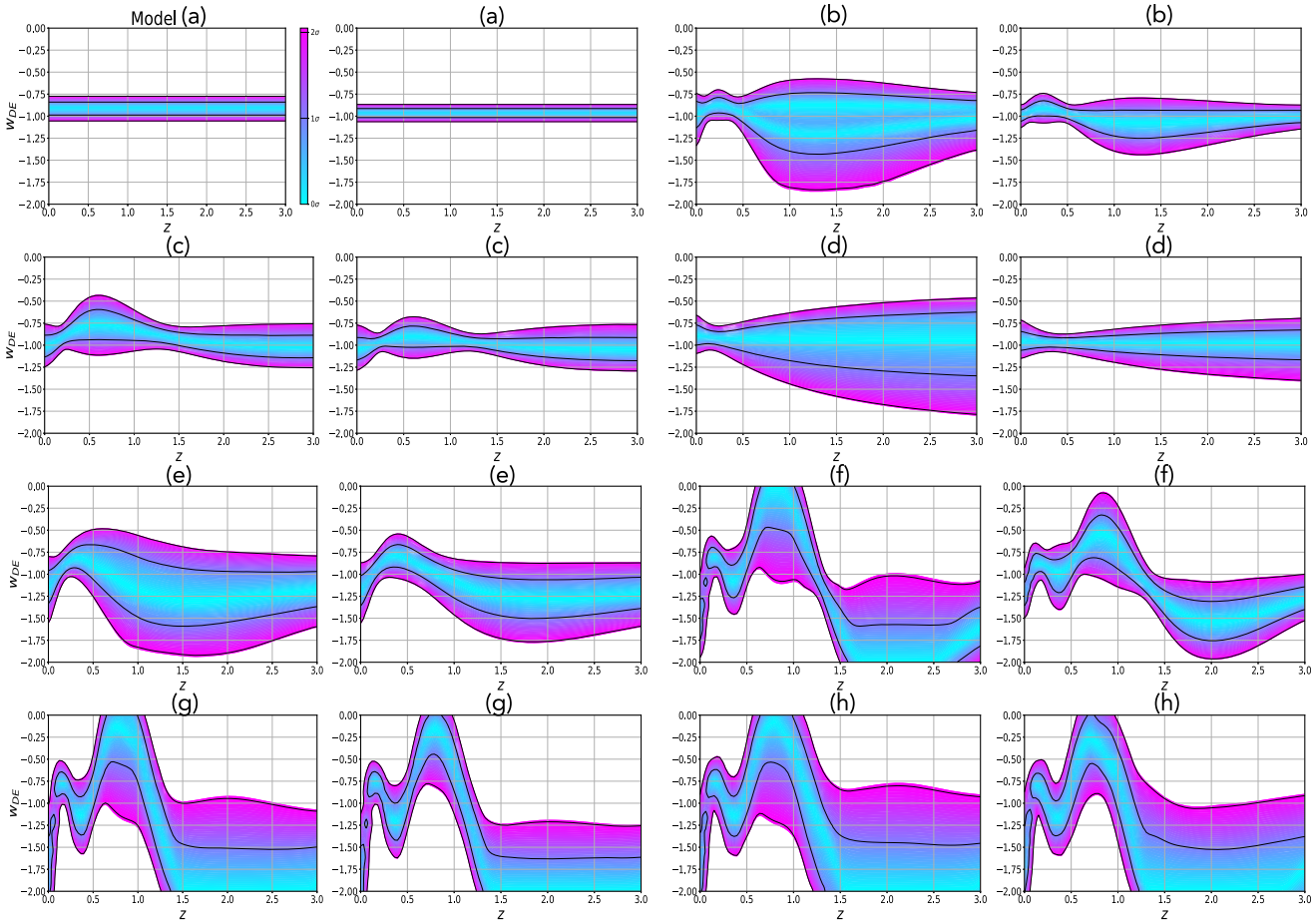

Figure 3. These plots show the posterior probability $\Pr(w|z)$: the probability of w as normalized in each slice of constant z, with the colour scale in confidence-interval values for the different cases shown in Table 1. The 1σ and 2σ confidence intervals are plotted as black lines. The left-hand panel for each case contains SN+BAO+HD data sets, while the right-hand panel additionally includes PLK data.

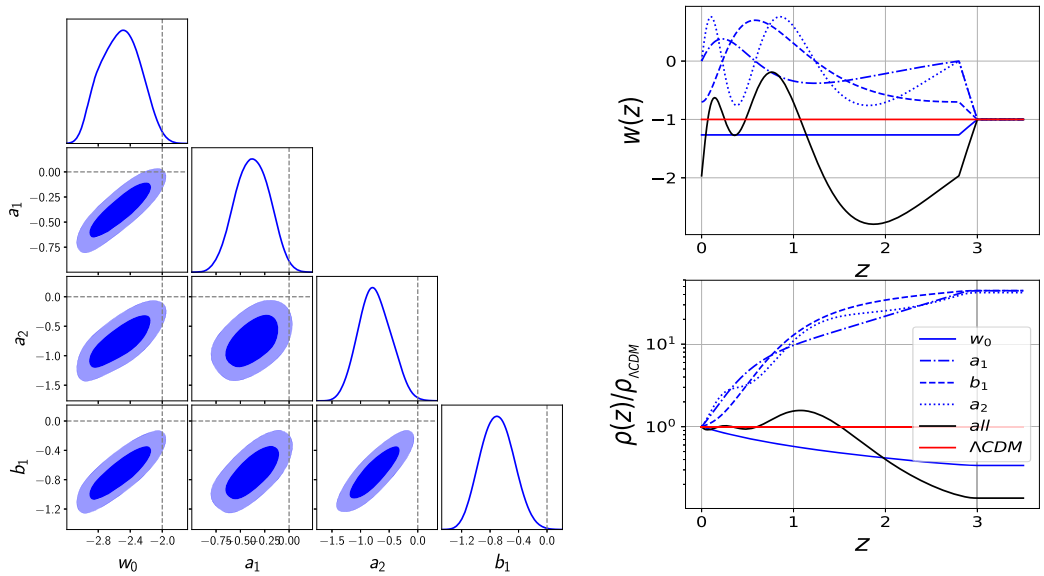

Figure 4. Left: 1D and 2D probability posterior distributions of the parameters used in model (g) with the incorporation of PLK data. Vertical dashed lines correspond to the ΛCDM values. Right: $w(z)$ and $\rho(z)$ contributions from each term in the Fourier expansion. The best-fitting values of the left-hand panel were used in this plot.

correct dark-energy model. If future surveys confirm its existence, single scalar field theories (with minimal assumptions) might be in serious trouble as they cannot reproduce this essential feature, and therefore alternative models should be considered. A key point to stress is that the cosmological constant $w = -1$ lays down far outside of the 2σ region (outer solid black line), particularly at high redshift on the second plot of model (g) of Fig. 3. The richness of this form is a consequence of releasing some tension between the data sets, especially for the high-z BAO.

Of all the models presented in Table 1, model (g) deviates the most from the cosmological constant (3.1σ). Fig. 4 displays 1D and 2D marginalized posterior distributions for the parameters used to describe model (g). The vertical dashed lines, which correspond to the ΛCDM model, give an insight into the amount of deviation that each parameter presents; in particular, parameters b_1 and a_2 deviate the most from the standard values. Here we also notice that some parameters are highly correlated. In future work we would perform a dimensional reduction analysis (i.e. Principal Component Analysis (PCA)), which decreases the penalty factor, but still preserves a similar shape of $w(z)$ and hence $-2\ln\mathcal{L}$ stays at a similar value. On the other hand, the right-hand panel of Fig. 4 displays the $w(z)$ and $\rho(z)$ contributions from each term in the Fourier expansion. The a_2 parameter contribution looks very similar to the full Fourier expansion, and hence its importance in the reconstruction. Similarly the b_1 parameter enhances the amplitude of the major peak and provides contributions to the low negative values of $w(z)$ and redshift today.

5 CONCLUSIONS AND DISCUSSIONS

In this work were proposed Fourier series to describe the dynamical dark-energy EoS parameter $w(z)$. This approach reproduces the oscillating behaviour of $w(z)$ shown in reconstructions from observational data. It also generalizes previous dynamical dark-energy proposals from trigonometrical functions and avoids some problems inherent to models based on the Taylor series, like the divergence at relative high redshift (∼3). For several selected cases of the Fourier series, the parameters were constrained from data using SIMPLEMC and compared with other models such as ΛCDM and a particular case of the Taylor series (the CPL model). We noticed that, as the number of parameters increases (i.e. terms of the series), more correlations amongst them are created, and also an increment to the penalization factor in the Akaike criterion occurs. The Fourier-series approach yields a better fit to the data by more than 3σ in comparison to the cosmological constant $w = -1$, therefore showing a clear preference for dynamical dark-energy behaviour. Moreover, if we compare the particular model (g) against the CPL parametrization, we find that model (g) is preferred by more than 3σ; also the difference in the Akaike criterion is $\Delta\mathrm{AIC_C} = -4.9$, which can be considered as strong evidence against the CPL description. With this analysis, in a model-independent way, we are able to discriminate the cosmological constant and provide a better fit than the Taylor expansion, in particular with the CPL parametrization. We have considered the $\mathrm{AIC_C}$ to penalize the extra parameters introduced in our analysis. Even though this penalization factor acts strongly, the criteria still tells us that a Fourier expansion provides a slightly better explanation of the data, especially for the inclusion of BAO at high redshift. This first analysis considering $w(z)$ as a Fourier series has its success in having a natural oscillatory behaviour and being compatible with model-independent reconstructions. More and better observational data are needed to test in more detail this proposal; however, it seems that multiple crosses of the PDL are unavoidable, putting in conflict some simple models for dark energy such as the cosmological constant, simple scalar fields, CPL and low-order Taylor series.

ACKNOWLEDGEMENTS

JAV acknowledges the support provided by FOSEC SEP-CONACYT Investigación Básica A1-S-21925, and DGAPA-PAPIIT IA102219. DT acknowledges financial support from CONACYT Mexico postdoctoral fellowships. The authors thank Josué De-Santiago for the revision of the manuscript.

REFERENCES

Ade P. A. R. et al., 2016, A&A, 594, A13
Akarsu z., Dereli T., Vazquez J. A., 2015, J. Cosmology Astroparticle Phys., 1506, 049
Alberto Vazquez J., Bridges M., Hobson M. P., Lasenby A. N., 2012, J. Cosmology Astroparticle Phys., 1209, 020
Arun K., Gudennavar S., Sivaram C., 2017, Advances Space Res., 60, 166
Aubourg E. et al., 2015, Phys. Rev. D, 92, 123516
Burnham K. P., Anderson D. R., 2002, Model Selection and Multimodel Inference: A Practical Information-Theoretic Approach, 2nd edn. Springer, Berlin
Chevallier M., Polarski D., 2001, Int. J. Mod. Phys. D, 10, 213
Clifton T., Ferreira P. G., Padilla A., Skordis C., 2012, Phys. Rep., 513, 1
Dai J.-P., Yang Y., Xia J.-Q., 2018, ApJ, 857, 9
Delubac T. et al., 2015, A&A, 574, A59
Gómez-Valent A., Amendola L., 2018, J. Cosmology Astroparticle Phys., 1804, 051
Hee S., Vazquez J. A., Handley W. J., Hobson M. P., Lasenby A. N., 2017, MNRAS, 466, 369
Jaime L. G., Jaber M., Escamilla-Rivera C., 2018, Phys. Rev. D, 98, 083530
Kumar S., Xu L., 2014, Phys. Lett. B, 737, 244
Kurek A., Hrycyna O., Szydlowski M., 2008, Phys. Lett. B, 659, 14
Linder E. V., 2003, Phys. Rev. Lett., 90, 091301
Linder E. V., 2006, Astroparticle Phys., 25, 167
López-Corredoira M., 2017, Foundations Phys., 47, 711
Martins C. J. A. P., Colomer M. P., 2018, A&A, 616, A32
Pace F., Fedeli C., Moscardini L., Bartelmann M., 2012, MNRAS, 422, 1186
Padilla A., 2015, preprint (arXiv:1502.05296)
Padilla L. E., Tellez L. O., Escamilla L. A., Vazquez J. A., 2019, preprint (arXiv:1903.11127)
Pan S., Saridakis E. N., Yang W., 2018, Phys. Rev. D, 98, 063510
Panotopoulos G., Rincón A., 2018, Phys. Rev. D, 97, 103509
Riess A. G. et al., 2016, ApJ, 826, 56
Sagredo B., Lafaurie J. S., Sapone D., 2018, preprint (arXiv:1808.05660)
Scherrer R. J., 2015, Phys. Rev. D, 92, 043001
Slosar A., 2014, Available at: https://github.com/slosar/april
Velten H. E. S., vom Marttens R. F., Zimdahl W., 2014, Eur. Phys. J. C, 74, 3160
Wang Y., Pogosian L., Zhao G.-B., Zucca A., 2018, ApJ, 869, L8
Yoo J., Watanabe Y., 2012, Int. J. Mod. Phys. D, 21, 1230002
Zhao G.-B. et al., 2017, Nat. Astron., 1, 627
Zimdahl W., 2012, AIP Conf. Proc., 1471, 51

This paper has been typeset from a TEX/LATEX file prepared by the author.